

Vibrational Spectroscopy

Elixir Vib. Spec. 91 (2016) 38368-38380

Elixir
ISSN: 2229-712X

Magnetic Properties and Vibrational Analysis of 2,3,4,5,6-Pentafluoroaniline-Quantum Chemical Approach

K.Sambathkumar^{a*}, A.Claude^a and K.Settu^a

^aDepartment of Physics, A.A.Government Arts College, Villupuram-605602.India.

ARTICLE INFO

Article history:

Received: 28 December 2015;

Received in revised form:

5 February 2016;

Accepted: 11 February 2016;

Keywords

FTIR,
FT-RAMAN,
PFA,
HOMO,
LUMO, TED.

ABSTRACT

The solid phase FTIR and FT-Raman spectra of 2,3,4,5,6-pentafluoroaniline(PFA) have been recorded in the region 4000-400 cm^{-1} and 3500-100 cm^{-1} , respectively. The spectra were interpreted with the aid of normal coordinate analysis following a full structure optimization and force field calculation based on the density functional theory (DFT) using the standard HF/6-31+G(d,p) and B3LYP/6-31+G(d,p) methods and basis set combination. A close agreement between the observed and calculated frequencies by refinement of the scale factor. The values of electric dipole moment (μ) and First-order hyperpolarizability(β) of the compound were computed using *ab-initio* quantum mechanical calculations. The calculation results also show that the PFA molecule might have microscopic nonlinear optical (NLO) behavior with non-zero values. HOMO and LUMO energy gap explains the eventual charge transfer interaction taking place within the molecule. Temperature dependence of various thermodynamic properties like heat capacity, enthalpy, Gibb's free energy, entropy is increase with increase in temperature. And magnetic susceptibility of the title compound at different temperatures is calculated.

© 2016 Elixir All rights reserved.

Introduction

Aniline and its derivatives have been widely used as starting materials in a vast amount of chemicals, pharmaceuticals, dyes, electro-optical and many other industrial processes [1-4]. The conducting polymer of aniline, namely, poly aniline is used in microelectronic devices as diodes and transistors [5-8]. Particularly, aniline and its derivatives are used in the production of dyes, pesticides and antioxidants. Consideration of these factors leads to undertake the detailed spectral investigation of 2,3,4,5,6-pentafluoroaniline (PFA). The aim of this work is to carry out an experimental and theoretical study on these compounds with the methods of quantum chemistry, in order to have a better understanding of its vibrational properties. However, for a proper understanding of IR and Raman spectra, reliable assignments of all vibrational bands are essential. Recently, computational methods based on density functional theory are being widely used. These methods predict a relatively accurate molecular structure and vibrational spectra with moderate computational effort. In particular, for polyatomic molecules, the DFT methods lead to the prediction of more accurate molecular structure and vibrational frequencies than the conventional *ab initio* restricted Hartree-Fock (HF) and Moller-Plesset second order perturbation theory (MP2) calculations [9- 12]. To the best of our knowledge, there is no theoretical calculations to understand the structure and the fundamental vibrational frequencies of PFA. This study is made to present a full description of the vibrational spectra of the title compounds, using *ab initio* HF and DFT (B3LYP) with 6-31+G(d,p) to obtain the geometries, vibrational frequencies, IR intensities and Raman activities. The atomic charges, distribution of electron density (ED) in various bonding and antibonding orbitals and stabilisation energies,

E(2) have been calculated by natural bond orbital (NBO) analysis.

Experimental Details

The spectroscopically pure grade sample of PFA are obtained from Lancsaster Chemical Company, UK and used as such for the spectral measurements.

The FTIR spectra of PFA is recorded in the region 4000 - 400 cm^{-1} at a resolution of $\pm 1 \text{ cm}^{-1}$ using BRUKER IFS 66V model FTIR spectrometer equipped with an MCT detector, a KBr beam splitter and globar arc source. The FT-Raman spectra of PFA is recorded using 1064 nm line of Nd:YAG laser as excitation wavelength in Stokes region (3500-100 cm^{-1}) on a BRUKER IFS-66 V model interferometer equipped with FRA-106 FT-Raman accessories operating at 200 mW power. The calibrated wave numbers are expected to be accurate within $\pm 1 \text{ cm}^{-1}$.

Computational Details

In order to provide information with regard to the structural characteristics and the normal vibrational mode of PFA, the Hartree-Fock and DFT-B3LYP correlation functional calculations have been carried out. The entire calculations are performed using the GAUSSIAN 09W software package [13]. Initially, the HF level calculations, adopting the 6-31+G(d,p) basis set are carried out and then the DFT employing the Becke 3LYP keyword, which invokes Becke's three-parameter hybrid method [20] has been computed using the correlation function of Lee *et al.* [14], implemented with the 6-31+G(d,p) basis set. All the parameters are allowed to relax and all the calculations converge to an optimized geometry which corresponds to a true minimum, as revealed by the lack of imaginary values in the wave number calculations. The Cartesian representation of the theoretical force constants has been computed at the fully optimized geometry. Transformation of force field, the

subsequent normal co-ordinate analysis including the least square refinement of the scale factors and calculations of Total energy (TED) are done on a PC with the MOLVIB program (version V7.0 – G77) and written by Sundius [15-17]. The symmetry of the mode is also helpful in making vibrational assignments by combining results of GAUSSVIEW Program with symmetry consideration, vibrational frequency assignments are made with a high degree of confidence. There is always some ambiguity in defining internal coordinate. However, the defined coordinate form complete set and matches quite well with the motions observed using the GAUSSVIEW program [18]. The systematic comparison of the results from DFT theory with results of experiments has been shown that the method using B3LYP functional is the most promising in providing correct vibrational wave numbers.

prediction of Raman Intensities

The Raman activities (S_i) calculated with the GAUSSIAN 09W program are subsequently converted to relative Raman intensities (I_i) using the following relationship derived from the basic theory of Raman scattering [19- 21],

$$I_i = \frac{f(v_0 - v_i)^4 S_i}{v_i \left[1 - \exp\left(-\frac{hc v_i}{kT}\right) \right]}$$

where v_0 is the exciting frequency in cm^{-1} , v_i the vibrational wave number of the i^{th} normal mode, h , c and k are the fundamental constants and f is a suitably chosen common normalization factor for all the peak intensities.

Results and Discussion

Molecular Geometry

The optimized molecular structure of PFA is shown in Fig.1, respectively. The optimization geometrical parameters of PFA obtained by the HF, DFT/ B3LYP with 6-31+G(d,p)

as basis set are listed in Table 1, respectively. The structural data provided in Table 1 indicate that various bond lengths are found to be almost same at HF/6-31+G(d,p) and B3LYP/6-31+G(d,p) levels. However, the B3LYP/6-31+G(d,p) level of theory, in general slightly overestimates the bond lengths but it yields bond angles in excellent agreement with the HF method. The calculated geometrical parameters are compared with X-ray diffraction results [22,23]

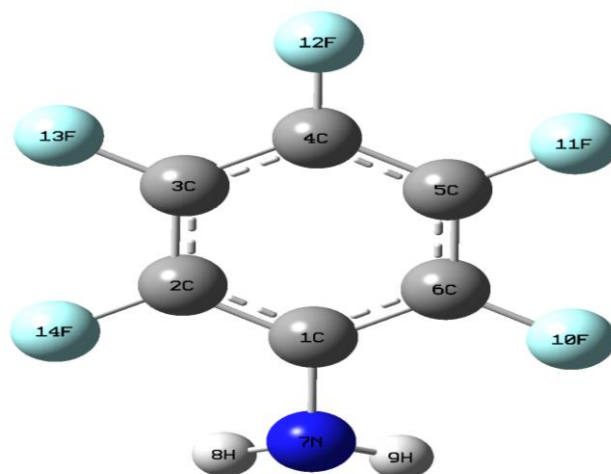


Fig 1. Molecular structure of 2,3,4,5,6-pentafluoroaniline

The calculated geometric parameters agree well with almost all values. The small deviations are probably due to the intermolecular interactions in the crystalline state of the molecule. Detailed description of vibrational modes can be given by means of normal coordinate analysis. The internal coordinates describe the position of the atoms in terms of distances, angles and dihedral angles with respect to an origin atom.

Table 1. Optimized geometrical parameters of 2,3,4,5,6-pentafluoroaniline obtained by using HF/6-31G+(d,p) and B3LYP/6-31G+(d,p) methods and basis set calculations

Bond length	Value (Å)		Exp	Bond angle	Value (°)		Exp	Dihedral Angle	Value (°)	
	HF/ 6-31G+(d,p)	B3LYP/6-31G+(d,p)			HF/6-31G+(d,p)	B3LYP/6-31G+(d,p)			HF/6-31G+(d,p)	B3LYP/6-31G+(d,p)
C1-C2	1.3864	1.4014	1.33(3)	C1-C2-C3	122.1273	122.3247	124.3(2)	C6-C1-C2-C3	-0.0402	0.2398
C2-C3	1.3763	1.3905	1.3371(3)	C2-C3-C4	120.0484	119.9877	116.5(2)	N7-C1-C2-C3	176.956	-176.839
C3-C4	1.3786	1.3938	1.369(4)	C3-C4-C5	119.1191	119.0943	123.6(2)	C2-C1-,6,5	0.0403	-0.2402
C4-C5	1.3786	1.3938	1.364(3)	C4-C5-C6	120.0484	119.9877	116.1(2)	C2-C1-6F14	-179.5686	179.3289
C5-C6	1.3763	1.3902	1.376(3)	C5-C6-C1	122.1273	122.3247	124.6(2)	N7-C1-C6-C5	-179.9559	176.8297
C6-C1	1.3640	1.4014	1.377(3)	C6-C1-C2	116.5288	116.2797	114.8(2)	N7-C1-6F14	3.4352	-3.6022
C1-N7	1.3799	1.3824	1.396(3)	C1-N7-8	115.5189	116.1791	114.6	C1-C2-C3-C4	-0.1179	0.0255
N7-H8	0.9954	1.0101	0.9009	C1-N7-H9	115.5189	166.1791	108.3	F10-C2-C3-C4	-179.724	179.5885
N7-H9	0.9954	1.0101	0.8798	H8-N7-H9	113.6822	114.6041	115.8	C2-C3-C4-C5	0.2744	-0.2980
C2-F10	1.3278	1.3537	1.358(3)	C6-C1-N7	122.1273	122.3247	122.5(2)	C2-C3-C4-F12	-179.996	179.8862
C4-F12	1.3188	1.3432	1.367(2)	C2-C1-N7	120.0484	119.9877	122.6(2)	C3-C4-C5-C6	-0.2744	0.2995
C6-F14	1.3278	1.3537	1.359(2)	C1-C2-F10	119.1191	119.0943	117.0(19)	F12-C4-C5-C6	179.9961	-179.886
C3-F11	1.3271	1.3530		C3-C2-F10	119.3041	119.4373	118.7(2)	C4-C5-C6-C1	0.1178	-0.0249
C5-F13	1.3178	1.3428		C3-C4-F12	120.4402	120.4527	117.9(2)	C4-C5-C6-F14	179.7239	-179.588
				C5-C4-F12	119.4401	120.4527	118.5(2)			
				C5-C6-F14	119.3041	119.4373	118.5(2)			
				C1-C6-F14	118.567	118.236	116.9(2)			

Table 2. Definition of internal coordinates of 2,3,4,5,6-pentafluoroaniline

No. (i)	Symbol	Type	Definition ^a
Stretching			
1	r _i	C-N	C1-N7
2 - 6	R _i	C-F	C2-F10, C3-F11, C4-F12, C5-F13, C6-F14
7 - 12	q _i	C-C	C1-C2, C2-C3, C3-C4, C4-C5, C5-C6, C6-C1
13, 14	p _i	N-H	N7-H8, N7-H9
In-plane bending			
15 - 20	α _i	Ring	C1-C2-C3, C2-C3-C4, C3-C4-C5, C4-C5-C6, C5-C6-C1, C6-C1-C2
21 - 30	β _i	C-C-F	C1-C2-F10, C3-C2-F10, C2-C3-F11, C4-C3-F11, C3-C4-F12, C5-C4-F12, C4-C5-F13, C6-C5-F13, C5-C6-F14, C1-C6-F14
31, 32	ν _i	C-C-N	C6-C1-N7, C2-C1-N7
33, 34	σ _i	C-N-H	C1-N7-H8, C1-N7-H9
35	δ _i	H-N-H	H8-N7-H9
Out-of-plane bending			
36- 40	ψ _i	C-F	F10-C2-C1-C3, F11-C3-C2-C4, F12-C4-C3-C5, F13-C5-C4-C6, F14-C6-C5-C1
41	μ _i	C-N	N7-C1-C2-C6
Torsion			
42 - 47	τ _i	t Ring	C1-C2-C3-C4, C2-C3-C4-C5, C3-C4-C5-C6, C4-C5-C6-C1, C5-C6-C1-C2, C6-C1-C2-C3
48	τ _i	t C-NH2	C1-N7-H8- H9

^aFor numbering of atoms refer Fig. 1

The symmetry coordinates are constructed using the set of internal coordinates. In this study, the full sets of 48 standard internal coordinates (containing 12 redundancies) for PFA are defined as given in Table 2. From these, a non-redundant set of local symmetry coordinates are constructed by suitable linear combinations of internal coordinates following the recommendations of Fogarsi *et al.* [24] and is summarized in Table 3. The theoretically calculated DFT force fields are transformed to this later set of vibrational coordinates and used in all subsequent calculations.

Using the DFT/B3LYP with large basis set calculations; several thermodynamic properties of PFA have been calculated. The values obtained for zero-point vibrational energy, rotational constants, rotational temperature, thermal energy, molar capacity at constant volume, entropy and dipole moment along with the global minimum energy are presented in Table 4 for PFA, respectively. The difference in the values calculated by the method is only marginal. The variation in the ZPVE seems to be insignificant. The total energy and the change in the total entropy of the molecule at room temperature are also presented

Vibrational Spectra

From the structural point of view the PFA is assumed to have C_s point group symmetry. Both the compounds 36 normal modes of vibrations are distributed among the symmetry species as

$$\overline{3N} - 6 = 25 A' \text{ (in-plane)} + 11 A'' \text{ (out-of-plane)}$$

The A' and A'' species represent the in-plane and out-of-plane vibrations, respectively. The detailed vibrational assignments of fundamental modes of PFA along with calculated IR, Raman intensities, force constants and normal mode descriptions (characterized by TED) are reported in Table 5. The FTIR and FT-Raman spectra of PFA are shown in Figs.2-3. The vibrational analysis obtained for

Table 3. Definition of local symmetry coordinates of 2,3,4,5,6-pentafluoroaniline

No. (i)	Type	Definition ^a
1	C N	r ₁
2-6	C F	R ₂ , R ₃ , R ₄ , R ₅ , R ₆
7-12	C C	q ₇ , q ₈ , q ₉ , q ₁₀ , q ₁₁ , q ₁₂
13	NH ₂ ss	(P ₁₃ + P ₁₄) / √2
14	NH ₂ ass	(P ₁₃ - P ₁₄) / √2
15	Ring trigd	(α ₁₅ - α ₁₆ + α ₁₇ - α ₁₈ + α ₁₉ - α ₂₀) / √6
16	Ring symd	(-α ₁₅ - α ₁₆ + 2α ₁₇ - α ₁₈ - α ₁₉ + 2α ₂₀) / √12
17	Ring asymd	(α ₁₅ - α ₁₆ + α ₁₈ - α ₁₉) / 2
18, 22	b C F	(β ₂₁ - β ₂₂) / √2, (β ₂₃ - β ₂₄) / √2, (β ₂₅ - β ₂₆) / √2, (β ₂₇ - β ₂₈) / √2, (β ₂₉ - β ₃₀) / √2
23	b C N	(ν ₃₁ - ν ₃₂) / √2
24	NH ₂ rock	(σ ₃₃ - σ ₃₄) / √2
25	NH ₂ twist	(σ ₃₃ + σ ₃₄) / √2
26	NH ₂ sciss	(2δ ₃₅ - σ ₃₃ - σ ₃₄) / √6
27-31	ψ C F	ψ ₃₆ , ψ ₃₇ , ψ ₃₈ , ψ ₃₉ , ψ ₄₀
32	μ C N	μ ₄₁
33	t Ring trigd	(τ ₄₂ - τ ₄₃ + τ ₄₄ - τ ₄₅ + τ ₄₆ - τ ₄₇) / √6
34	t Ring symd	(τ ₄₂ - τ ₄₄ + τ ₄₅ - τ ₄₇) / √2
35	t Ring asymd	(-τ ₄₂ + 2τ ₄₃ - τ ₄₄ - τ ₄₅ + 2τ ₄₆ - τ ₄₇) / √12
36	t C-NH ₂ wag	τ ₄₈

PFA with the unscaled HF and B3LYP/ 6-31+G(d,p) force field are generally somewhat greater than the experimental values due to neglect of anharmonicity in real system. These discrepancies can be corrected either by computing anharmonic corrections explicitly or by introducing a scaling the calculated wavenumbers with proper scale factor. Then, for an easier comparison to the observed values, the calculated frequencies are scaled to less than 1, to minimize the overall deviation. Therefore, we have used the different scaling factor values of HF/6-31+G(d,p) methods. The results indicate that the B3LYP calculations approximate the observed fundamental frequencies much better than the HF results. Inclusion of electron correlation in density functional theory to a certain extent makes the frequency values smaller in comparison with HF frequency. Also, it should be noted that the experimental results belong to solid phase and theoretical calculations belong to gaseous phase. The resultant scaled frequencies are also listed in Table 6.

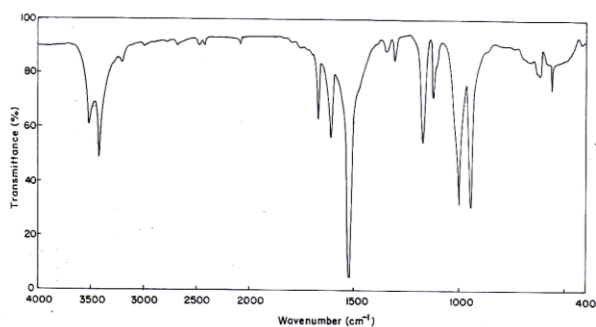


Fig 2.FTIR spectrum of 2,3,4,5,6-pentafluoroaniline

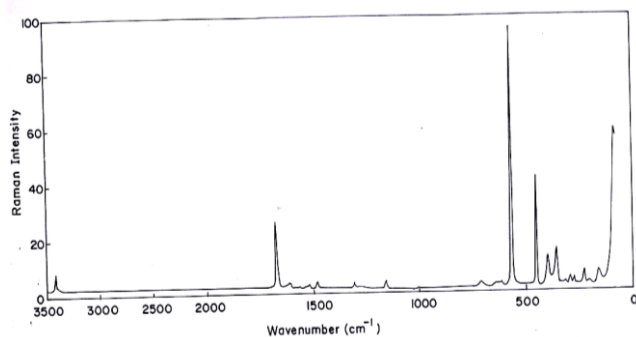


Fig 3. FT-Raman spectrum of 2,3,4,5,6-pentafluoroaniline

C–C Vibrations

The C–C aromatic stretching vibrations gives rise to characteristic bands in the observed IR and Raman spectra, covering the spectral range from 1650 to 1400 cm^{-1} . Therefore, the C–C stretching vibrations of PFA are observed at 1820, 1760, 1658, 1612, 1525 cm^{-1} and 1649, 1614 cm^{-1} in FTIR and FT-Raman spectrum, respectively. Most of the ring vibrational modes are affected by the substitutions in the aromatic ring of PFA [25]. The FTIR and Raman spectrum have been designated to ring in-plane bending modes by careful consideration of their quantitative descriptions. The ring out-of-plane bending modes of PFA are also listed in Table 5. The reductions in the frequencies to these modes are due to the change in force constant and the vibrations of the functional groups present in the molecule. The theoretically computed values for C–C vibrational modes by B3LYP/6-31+G(d,p) method gives excellent agreement with experimental data.

Table 4. The thermodynamic parameters of 2,3,4,5,6-pentafluoroaniline along with the global minimum energy calculated at HF/6-31+G(d,p) and B3LYP/6-31+G(d,p) methods

Parameters	B3LYP/ 6-31+G(d,p)
Optimized global minimum energy (Hartees)	-783.7957
Zero-point vibrational energy(kcal mol ⁻¹)	47.9052
Rotational constants (GHz)	1.0346
	1.0194
	0.5136
Rotational temperature (Kelvin)	0.0496
	0.0489
	0.0246
Energy (kcal mol ⁻¹)	
Total	54.369
Translational	0.899
Rotational	0.889
Vibrational	52.592
Molar capacity at constant Volume (cal mol ⁻¹ Kelvin)	
Total	38.313
Translational	2.9812
Rotational	2.9812
Vibrational	32.352
Entropy(cal mol ⁻¹ Kelvin)	
Total	98.188
Translational	41.520
Rotational	30.762
Vibrational	25.906
Dipole moment(Debye)	
μ_x	-1.1093
μ_y	-0.3093
μ_z	-0.6403
μ_{total}	1.7363

Table 5. The observed (FTIR and FT-Raman) and calculated (unscaled and scaled) frequencies (cm^{-1}), IR intensity (km mol^{-1}), Raman activity ($\text{\AA} \text{amu}^{-1}$) and force constant (m dyne \AA) and probable assignments (Characterized by TED) of 2,3,4,5,6-pentafluoroaniline using HF/6-31+G(d,p) and B3LYP/6-31+G(d,p) calculations

Symmetry species C_s	Observed frequencies (cm^{-1})		Calculated frequencies (cm^{-1}) (Unscaled)		Scaling frequency (cm^{-1})		Force constant (mDyne/ \AA)		IR intensity (KM/Mole)		Raman activity ($\text{\AA}^4/\text{amu}$)		Assignments (% TED)
	FTIR	FT-Raman	HF	B3LYP	HF	B3LYP	HF	B3LYP	HF	B3LYP	HF	B3LYP	
A'	3614(ms)	-	3971	3805	3835	3616	10.032	8.9131	57.107	49.893	38.096	41.408	NH ₂ ass (98)
A'	-	3520(w)	3894	3867	3819	3523	8.9873	7.9480	63.7670	61.446	118.95	156.29	NH ₂ ss (96)
A'	1820(vw)	-	1961	1899	1861	1823	15.432	11.4788	27.8864	55.642	44.856	42.954	v CC (92)
A'	1760(w)	-	1938	1863	1842	1764	20.182	16.5029	3.4059	3.1165	1.0889	2.0690	vCC (81), vCF (15)
A'	1658(ms)	-	1893	1842	1798	1659	2.3103	1.9931	88.4608	68.557	0.8666	0.0877	vCC (83), vCF (14)
A'	-	1649(vw)	1783	1723	1708	1653	17.145	13.2670	371.818	357.32	0.0520	0.9449	vCC (82), vCF (11)
A'	1612(s)	1614(ms)	1765	1683	1723	1619	17.913	13.9531	362.432	306.001	3.0918	0.0596	vCC (87), vCF (14)
A'	-	1601(ms)	1739	1665	1643	1605	16.237	14.3961	27.9045	1.2806	11.154	3.2945	NH ₂ sciss (60), vCC (22)
A'	1525(vs)	-	1658	1634	1614	1529	13.156	7.5614	1.6471	6.2226	0.4546	3.0397	vCC (84), vCF (14)
A'	1360(m)	1360(vw)	1546	1522	1490	1364	2.2342	10.7376	32.7130	3.5185	3.5825	0.4545	vCF (59), NH ₂ sciss (26)
A'	1352(w)	-	1475	1419	1390	1355	8.6871	1.8670	4.0353	89.9506	2.0180	0.6460	vCF (72), vCC (12)
A'	1345(ms)	-	1452	1401	1387	1348	6.1927	7.4057	23.6343	0.5788	0.0042	3.6177	vCF (63), vCC (17)
A'	1322(ms)	1320(w)	1389	1368	1355	1324	6.0157	4.3651	104.495	42.7463	1.6307	0.0666	vCF (61), vCC (22)
A'	1310(ms)	-	1371	1369	1356	1314	7.5217	6.8083	240.416	213.000	0.4779	0.2637	vCF (58), vCN (24)
A'	1180(s)	1182(vw)	1298	1255	1230	1183	3.1335	2.6723	174.317	165.244	0.0983	0.2605	vCN (57), vCF (28)
A'	1110(ms)	-	1183	1159	1143	1118	2.3786	1.9819	0.0012	0.0000	0.0238	0.0287	NH ₂ rock (55), bCF (25)
A'	1010(vs)	-	1099	1078	1064	1017	3.3871	3.1387	13.2480	1.9228	1.1595	1.7372	bCF (75), bCN (18)
A'	-	1000(vw)	1056	1034	1025	1009	3.6479	2.8729	0.0618	0.0013	0.0199	0.0539	bCF (76), NH ₂ rock (12)
A'	910(vs)	-	1001	978	967	919	3.5799	2.8607	0.4575	0.1823	0.6347	0.4800	bCF (64), R asymd (17)
A'	870(vw)	-	990	970	955	878	0.8805	1.4425	85.0504	24.1454	2.8048	3.4938	bCN (68), R symd (13)
A'	-	854(vw)	891	878	866	860	2.5937	2.6208	5.8528	1.5341	26.633	33.317	bCF (60), R trigd (14)
A'	790(w)	-	867	854	823	797	0.3810	0.2086	240.094	296.019	4.4611	2.9105	bCF (72), t R asymd (19)
A'	-	712(w)	787	759	740	719	1.6890	1.4611	0.4068	0.6689	4.8768	5.3264	R asymd(53), bCF(26)
A'	680(w)	-	754	748	720	669	2.0880	1.7733	0.0137	0.0026	4.9563	5.3527	R symd(60), bCF (22)
A'	-	650(w)	712	699	675	658	1.3537	0.4519	0.1170	1.8443	3.3098	2.4175	R trigd (74), bCF(16)
A''	610(ms)	-	692	678	667	618	0.8522	0.6236	9.6935	5.8966	2.7781	2.1851	ω CF(62), bCF (26)
A''	-	583(vs)	634	612	601	594	1.1114	0.0878	2.8800	9.5600	0.0452	1.2946	ω CF (67), t R symd(28)
A''	570(ms)	573(s)	599	588	582	577	0.5652	0.9319	1.6091	1.7641	0.1297	0.4051	ω CF (61), t R trigd(20)
A''	460(w)	-	578	534	520	471	0.0876	0.4545	8.3926	0.2582	0.7142	0.0342	t R asymd (59), ω CF(22)
A''	-	394(vw)	550	535	510	408	0.1650	0.2070	9.9565	5.3962	0.0555	0.1538	t R symd(58), ω CF(24)
A''	-	253(m)	534	502	478	306	0.9487	0.7910	0.0441	0.0614	0.0519	0.1362	t R trigd (60)
A''	-	190(s)	490	465	394	298	0.2490	0.3460	5.4282	2.2052	0.1201	0.3809	ω CN (57)
A''	-	-	336	309	290	280	0.3613	0.2776	2.9709	1.4469	0.2316	0.3077	ω CF (55)
A''	-	-	306	287	260	250	0.2763	0.2322	1.2780	1.0252	0.1008	0.1739	ω CF (53)
A''	-	-	252	237	212	156	0.2543	0.2044	0.0040	0.0049	0.0028	0.0033	NH ₂ wag (68)
A''	-	-	298	256	231	153	0.1139	0.0986	2.1113	1.7169	0.2131	0.3349	NH ₂ twist (52)

Abbreviations: v - stretching; b - in-plane bending; ω - out-of-plane bending; asymd - asymmetric; symd - symmetric; t - torsion; trig - trigonal; w - weak; vw-very weak; vs - very strong; s - strong; ms - medium strong; ss - symmetric stretching; ass - asymmetric stretching; ips - in-plane stretching; ops - out-of-plane stretching; sb - symmetric bending; ipr - in-plane rocking; opr - out-of-plane rocking; opb - out-of-plane bending.

Table 6. Calculated atomic charges of 2,3,4,5,6-pentafluoroaniline by natural bond orbital (NBO) analysis by B3LYP method

Atom No	Charge	Core	Valence	Total
C1	0.02233	1.99880	3.96030	5.97767
C2	0.35442	1.99829	3.62026	5.64558
C3	0.30565	1.99837	3.66974	5.69435
C4	0.30596	1.99837	3.66958	5.69404
C5	0.30447	1.99837	3.67090	5.69553
C6	0.33805	1.99829	3.63797	5.66195
N7	-0.88853	1.99964	5.86661	7.88853
H8	0.41608	0.00000	0.58125	0.58392
H9	0.41661	0.00000	0.58112	0.58339
F10	0.31104	1.99994	7.30062	9.31104
F11	-0.31358	1.99994	7.30287	9.31358
F12	-0.31179	1.99994	7.30089	9.31179
F13	-0.31524	1.99994	7.30466	9.31524
F14	-0.32340	1.99994	7.31282	9.32340

Table 7. The atomic orbital occupancies of 2,3,4,5,6-pentafluoroaniline

Atom No	Atomic orbital	Type	Occupancy	Energy
C1	1s	Core	0.99940	10.14536
	2s	Valence	0.44584	0.23269
	2p _x	Valence	0.47275	-0.11248
	2p _y	Valence	0.53060	-0.11135
	2p _z	Valence	0.53095	-0.16892
C2	1s	Core	0.99915	-10.20042
	2s	Valence	0.42542	-0.23257
	2p _x	Valence	0.51258	-0.10535
	2p _y	Valence	0.34935	-0.09673
	2p _z	Valence	0.52278	-0.17868
C3	1s	Core	0.99919	-10.20756
	2s	Valence	0.43431	-0.25019
	2p _x	Valence	0.43487	-0.10896
	2p _y	Valence	0.43006	-0.11042
	2p _z	Valence	0.53563	-0.18543
C4	1s	Core	0.99919	-10.21097
	2s	Valence	0.43370	-0.25289
	2p _x	Valence	0.34698	-0.10652
	2p _y	Valence	0.51766	-0.11762
	2p _z	Valence	0.53645	-0.18748
C5	1s	Core	0.99919	-10.20802
	2s	Valence	0.43431	-0.25075
	2p _x	Valence	0.51633	-0.11580
	2p _y	Valence	0.34845	-0.10563
	2p _z	Valence	0.53635	-0.18633
C6	1s	Core	0.99914	-10.20189
	2s	Valence	0.42548	-0.23595
	2p _x	Valence	0.43081	-0.10953
	2p _y	Valence	0.43323	-0.10339
	2p _z	Valence	0.52947	-0.18352
N7	1s	Core	0.99982	-14.21866
	2s	Valence	0.71020	-0.59815
	2p _x	Valence	0.61486	-0.21718
	2p _y	Valence	0.86395	-0.25736
	2p _z	Valence	0.74430	-0.23419
H 8	1s	Valence	0.29062	0.13474
H9	1s	Valence	0.29056	0.12815
F10	1s	Core	0.99997	-24.49079
	2s	Valence	0.91555	-1.30968
	2p _x	Valence	0.96760	-0.44540
	2p _y	Valence	0.80659	-0.45257
	2p _z	Valence	0.96057	-0.44564
F11	1s	Core	0.99997	-24.49698
	2s	Valence	0.91611	-1.31412
	2p _x	Valence	0.88940	-0.45394
	2p _y	Valence	0.88396	-0.45396
	2p _z	Valence	0.96197	-0.45022
F12	1s	Core	0.99997	-24.49977
	2s	Valence	0.91623	-1.31639
	2p _x	Valence	0.80233	-0.45924
	2p _y	Valence	0.96985	-0.45310
	2p _z	Valence	0.96203	-0.45242
F13	1s	Core	0.99997	-24.49793
	2s	Valence	0.91607	-1.31544
	2p _x	Valence	0.96870	-0.45240
	2p _y	Valence	0.80535	-0.45837
	2p _z	Valence	.96220	-0.45159
F14	1s	Core	0.99997	24.50178
	2s	Valence	0.91519	1.32331
	2p _x	Valence	0.89041	-0.46356
	2p _y	Valence	0.88816	-0.46297
	2p _z	Valence	0.96265	-0.45904

C–F vibrations

In the vibrational spectra of PFA, the bands due to the C–F stretching vibrations may be found over a wide frequency range 1360 – 1000 cm^{-1} [25], since the vibration is easily affected by adjacent atoms (or) groups. In the present investigation, the FTIR and FT-Raman bands observed at 1360, 1352, 1345, 1322, 1310 cm^{-1} and 1360, 1320 cm^{-1} have been assigned to C–F stretching modes of vibrations. The C–F in-plane and out-of-plane bending vibrations are observed at 1010, 910, 790 cm^{-1} in IR and 1000, 854 cm^{-1} in Raman and 610, 570 cm^{-1} in IR and 583, 573 cm^{-1} in Raman, respectively.

C–N vibrations

The identification of C–N stretching frequency is a very difficult task. Since the mixing of bands are possible in this region 1200 – 1400 cm^{-1} . However, with the help of force field calculations the C–N vibrations are identified and assigned in this study. The FTIR band observed at 1180 cm^{-1} and the Raman band at 1182 cm^{-1} in PFA are assigned to C–N stretching modes of vibrations. The band appeared at 870 cm^{-1} in IR has been designated to C–N in-plane bending vibration and the band found at 190 cm^{-1} are assigned to out-of-plane bending vibrations made in this study are also supported by the literature [25].

NH₂ Vibrations

The molecule under consideration possesses NH₂ group and hence six internal modes of vibration are possible such as symmetric stretching, asymmetric stretching, scissoring, rocking, wagging and the torsional mode. The NH₂ group has two (N–H) stretching vibrations; one being asymmetric and the other symmetric. The frequency of asymmetric vibration is higher than that of symmetric one. The frequencies of amino group in the region 3500 – 3300 cm^{-1} for NH stretching, 1700 – 1600 for scissoring and 1150–900 for rocking deformation. In the present investigation, the asymmetric and symmetric modes of NH₂ group so the bands observed at 3614 cm^{-1} in FTIR, 3520 cm^{-1} in Raman have been assigned to NH₂ asymmetric and symmetric stretching modes of PFA. The bands appeared at 1601 cm^{-1} in Raman for PFA have been assigned to scissoring mode of NH₂ group. The rocking, wagging, twisting deformation vibrations of NH₂ contribute to several normal modes in the low frequency region. The band observed at 1110 cm^{-1} in FTIR for PFA cm^{-1} are assigned to NH₂ rocking vibrations [25].

Vibrational contribution to NLO activity and first hyperpolarizability

The potential application of the PFA in the field of nonlinear optics demands the investigation of its structural and bonding features contributing to the hyperpolarizability enhancement, by analyzing the vibrational modes using IR and Raman spectroscopy. The ring stretching bands of PFA observed at 1820, 1760, 1658, 1612, 1525 cm^{-1} in IR and have their counterparts in the Raman spectrum at 1649, 1614 cm^{-1} , respectively and their relative intensities in IR and Raman spectrum are comparable. The first hyperpolarizability (β) of this novel molecular system is calculated using the *ab-initio* HF method, based on the finite-field approach. In the presence of an applied electric field, the energy of a system is a function of the electric field. The first hyperpolarizability is a third-rank tensor that can be described by a $3 \times 3 \times 3$ matrix. The 27 components of the 3D matrix can be reduced to 10 components due to the Kleinman symmetry [26]. The

components of β are defined as the coefficients in the Taylor series expansion of the energy in the external electric field. When the electric field is weak and homogeneous, this expansion becomes

$$E = E_0 - \sum_i \mu_i F^i - \frac{1}{2} \sum_{ij} \alpha_{ij} F^i F^j - \frac{1}{6} \sum_{ijk} \beta_{ijk} F^i F^j F^k - \frac{1}{24} \sum_{ijkl} \nu_{ijkl} F^i F^j F^k F^l$$

where E_0 is the energy of the unperturbed molecule; F^i is the field at the origin; and μ_i , α_{ij} , β_{ijk} and ν_{ijkl} are the components of dipole moment, polarizability, the first hyper polarizabilities and second hyperpolarizabilities, respectively. The total static dipole moment μ , the mean polarizability α_0 and the mean first hyperpolarizability β_0 , using the x , y , z components they are defined as:

$$\mu = (\mu_x^2 + \mu_y^2 + \mu_z^2)^{1/2}$$

$$\alpha_0 = \frac{(\alpha_{xx} + \alpha_{yy} + \alpha_{zz})}{3}$$

$$\alpha = 2^{-1/2} \left[(\alpha_{xx} - \alpha_{yy})^2 + (\alpha_{yy} - \alpha_{zz})^2 + (\alpha_{zz} - \alpha_{xx})^2 + 6\alpha_{xx}^2 \right]^{1/2}$$

$$\beta_0 = (\beta_x^2 + \beta_y^2 + \beta_z^2)^{1/2}$$

$$\text{and } \beta_x = \beta_{xxx} + \beta_{yyy} + \beta_{zzz}$$

$$\beta_y = \beta_{yyy} + \beta_{xxy} + \beta_{yzz}$$

$$\beta_z = \beta_{zzz} + \beta_{xzx} + \beta_{yyz}$$

The calculated mean first hyperpolarizability (β) of the title compounds PFA are 0.5195×10^{-30} esu, respectively, which are comparable with the reported values of similar derivatives [25,26]. The large value of hyperpolarizability β which is a measure of the non-linear optical activity of the molecular system is associated with the intermolecular charge transfer, resulting from the electron cloud movement through π conjugated frame work from electron donor to electron acceptor groups. The physical properties of these conjugated molecules are governed by the high gaps. So, we conclude that the title compounds are an attractive object for future studies of nonlinear optical properties.

Homo-Lumo Analysis

Many organic molecules, containing conjugated π electrons are characterized by large values of molecular first hyper polarizabilities, and they are analyzed by means of vibrational spectroscopy [27]. In most of the cases, even in the absence of inversion symmetry, the strongest band in the Raman spectrum is weak in the IR spectrum and vice-versa. But the intramolecular charge from the donor to acceptor group through a single-double bond conjugated path can induce large variations of both the molecular dipole moment and the molecular polarizability, making IR and Raman activity strong at the same time. The experimental spectroscopic behaviour described above is well accounted for DFT calculations in π conjugated system that predict exceptionally infrared intensities for the same normal modes [52]. The analysis of the wave function indicates that the electron absorption corresponds to the transition from the ground to the first excited state and is mainly described by one-electron excitation from the highest occupied molecular orbital (HOMO) to the lowest unoccupied orbital (LUMO).

The LUMO; of π nature, (i.e. benzene ring) is delocalized over the whole C–C bond.

By contrast, the HOMO is located over NH_2 atoms; consequently the HOMO \rightarrow LUMO transition implies an electron density transfer to aromatic part and NH_2 of π conjugated system from benzene ring. Moreover, these three orbital's significantly overlap in the Para position of the benzene ring for CDBA and PFA. The atomic orbital compositions of the frontier molecular orbital are shown in Fig. 4. The HOMO \rightarrow LUMO energy gap of CDBA is calculated using HF/6-31+G(d,p) and B3LYP/6-31+G(d,p) level, reveals that the energy gap reflects the chemical activity of the molecules. The LUMO as an electron acceptor (EA) represents the ability to obtain an electron (ED), and HOMO represents the ability to donate an electron (ED). The ED groups to the efficient EA groups through π -conjugated path. The strong charge transfer interaction through π -conjugated bridge results insubstantial ground state donor-Acceptor (DA) mixing and the appearance of a charge transfer band in the electron absorption spectrum.

For PFA,

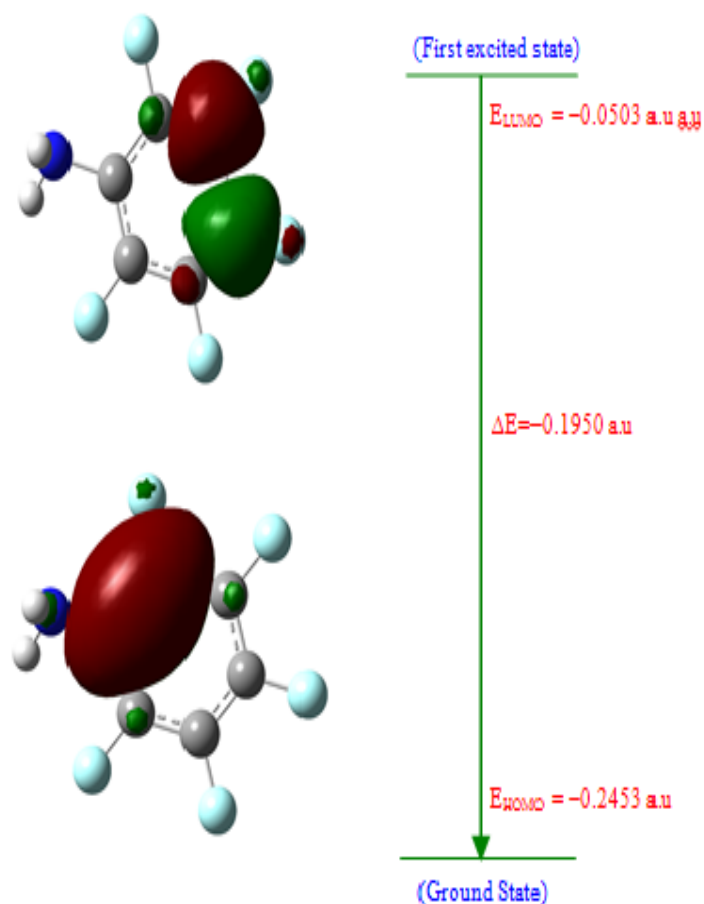


Fig 4. HOMO-LUMO of 2,3,4,5,6-pentafluoroaniline

	HF	B3LYP
HOMO energy	-0.3407 a.u	-0.2453 a.u
LUMO energy	-0.0520 a.u	-0.0503 a.u
Energy gap(ΔE)	-0.2887 a.u	-0.1950 a.u

The HOMO-LUMO energy gap explains the fact that eventual charge transfer interaction is taking place within the molecule.

Natural Bond Orbital Analysis

Natural bond orbital (NBO) methods encompass a suite of algorithms that enable fundamental bonding concepts to be

extracted from Hartree-Fock (HF), Density Functional Theory (DFT) and post-HF computations.

NBO analysis originated as a technique for studying hybridisation and covalency effects in polyatomic wave functions, based on local block eigen vectors of the one-particle density matrix. NBOs would correspond closely to the picture of localised bonds and lone pairs as basic units of molecular structure. The atomic charges, core, valences and total charge of PFA calculated by NBO analysis using the B3LYP/6-31+G(d,p) method are presented in Table 6. Among the ring carbon atoms C3 and C4 for PFA have same negative charges. But N7 has more negative charge due to the resonance of amino group for PFA. The both charges of H9 for PFA are same. In Table 7, the natural atomic orbitals, their occupancies and the corresponding energy of PFA are described. In a given molecular environment the natural atomic orbitals reflect the chemical give and take of electronic interactions, with variations of shape (e.g., angular deformations due to steric pressures of adjacent atoms) and size (e.g., altered diffuseness due to increased 250 anionic or cationic characters) that distinguish them appreciably for free atom forms. The NAOs orbital energies $\epsilon_i^{(A)}$ are calculated by using Kohn-Sham operator (F) as

$$\epsilon_i^{(A)} = \langle \theta_i^{(A)} | F | \theta_i^{(A)*} \rangle$$

The NAOs deals the molecular properties in terms of inter atomic and intra atomic contributions. The Table 8 depicts the bonding concepts such as type of bond orbital, their occupancies, the natural atomic hybrids of which the NBO is composed, giving the percentage of the NBO on each hybrid, the atom label, and a hybrid label showing the hybrid orbital (sp^x) composition (the amount of s -character, p -character, etc.,) of PFA molecule determined by B3LYP/6-31+G(d,p) method with respectable accuracy. The lone pair orbital structure of sp^2 is represented in Fig. 5 for PFA. The occupancies of NBOs in PFA reflect their exquisite dependence on the chemical environment.

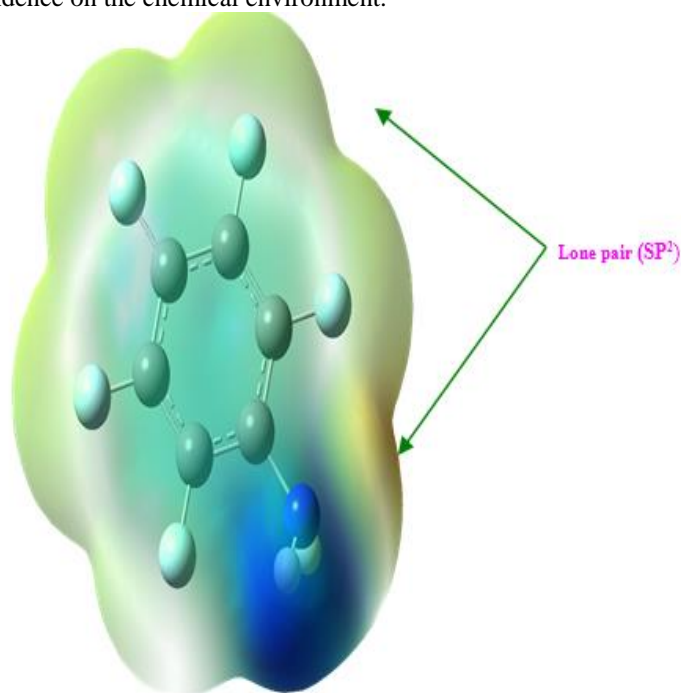


Fig 5. The lone pair structure of 2,3,4,5,6-pentafluoroaniline

The NBO energy values show the corresponding spatial symmetry breaking in the direction of unpaired spin. The

Lewis structure that is closest to the optimised structure is determined. The hybridisation of the atoms and the weight of each atom in each localised electron pair bond is calculated in this idealised Lewis structure and presented in Table 8.

Table 8. Bond orbital analysis of 2,3,4,5,6-pentafluoroaniline by B3LYP/ 6-31+G(d,p) method

Bond orbital	Occupancy	Atom	Contribution from parent NBO (%)	Coefficients	Atom Hybrid Contributions (%)
C1-C2	0.98681	C1	50.79	0.7127	s(35.64) + p 1.80(64.32)
		C2	49.21	0.7015	s(38.78) + p 1.58(61.18)
C1-C6	0.98752	C1	50.52	0.7108	s(35.40) + p 1.82(64.56)
		C6	49.48	0.7034	s(38.86) + p 1.57(61.10)
C1-N7	0.99298	C1	43.26	0.6577	s(28.80) + p 2.47(71.12)
		N7	56.74	0.7533	s(28.08) + p 2.56(71.85)
C2-C3	0.98989	C2	49.84	0.7060	s(36.88) + p 1.71(63.07)
		C3	50.16	0.7082	s(38.15) + p 1.62(61.81)
C2-F10	0.99728	C2	28.68	0.5356	s(24.15) + p 3.13(75.61)
		F10	71.32	0.8445	s(28.31) + p 2.53(71.58)
C3-C4	0.98919	C3	49.95	0.7068	s(37.67) + p 1.65(62.28)
		C4	50.05	0.7075	s(37.82) + p 1.64(62.14)
C3-F11	0.99725	C3	28.72	0.5360	s(24.00) + p 3.16(75.76)
		F11	71.28	0.8442	s(28.12) + p 2.55(71.76)
C4-C5	0.98911	C4	50.00	0.7071	s(37.79) + p 1.64(62.16)
		C5	50.00	0.7071	s(37.73) + p 1.65(62.23)
C4-F12	0.99714	C4	28.78	0.5365	s(24.22) + p 3.12(75.55)
		F12	71.22	0.8439	s(28.00) + p 2.57(71.89)
C5-C6	0.98973	C5	50.06	0.7076	s(38.16) + p 1.62(61.80)
		C6	49.94	0.7066	s(36.98) + p 1.70(62.97)
C5-F13	0.99729	C5	28.69	0.5356	s(23.94) + p 3.17(75.83)
		F13	71.31	0.8445	s(28.19) + p 2.54(71.69)
C6-F14	0.99740	C6	28.33	0.5323	s(23.97) + p 3.16(75.79)
		F14	71.67	0.8466	s(28.83) + p 2.46(71.06)
N7-H8	0.99415	N7	70.92	0.8422	s(27.63) + p 2.62(72.30)
		H8	29.08	0.5392	s(99.89) + p 0.00(0.11)
N7-H9	0.98965	N7	70.83	0.8416	s(25.97) + p 2.85(73.96)
		H9	29.17	0.5401	s(99.89) + p 0.00(0.11)

For CDBA and PFA, no antibonding orbitals are listed so that the structure is adequately explained by normal Lewis

electron pair orbitals. For example, the bonding orbital for C1–N7 with 0.99298 electrons has 43.26% C1 character in a *sp* 2.47 hybrid and has 56.74 % N7 character in a *sp* 2.56 hybrid orbital of PFA. The bonding orbital C2–F10 with 0.99728 electrons has 28.68% C2 character in a *sp* 3.13 hybrid and has 71.32% F10 character in a *sp* 2.53 hybrid orbital for PFA. A bonding orbital for C3–C4 with 0.98919 electrons has 49.95% C3 character in a *sp* 1.65 hybrid and has 50.05% C4 character in a *sp* 1.64 hybridised orbital for PFA [28].

Donor Acceptor Interactions: Perturbation Theory Energy Analysis

The localised orbitals in the Lewis structure of PFA can interact strongly. A filled bonding or lone pair orbital can act as a donor and an empty or filled bonding, antibonding, or lone pair orbital can act as an acceptor. These interactions can strengthen and weaken bonds. For example, lone pair donor → antibonding acceptors orbital interaction may 251 weaken the bond associated with the antibonding orbital.

Table 9. Second order perturbation theory analysis of Fock matrix of 2,3,4,5,6-pentafluoroaniline by NBO method

Donor (i) → Acceptor (j)	E ^{(2)a} (kJ mol ⁻¹)	E(j) – E(i) ^b (a.u.)	F(i, j) ^c (a.u.)
π C1-C2 → π* C3-C4	42.2166	0.27	0.068
π C1-C2 → π* C5-C6	42.0074	0.27	0.068
σ C1-C6 → σ* C2-F10	7.23832	1.00	0.053
σ C1-C6 → σ* C5-F13	7.44752	0.99	0.053
π C3-C4 → σ* C1-C2	38.451	0.30	0.068
π C3-C4 → π* C5-C6	39.3714	0.29	0.068
σ C4-C5 → σ* C6-F14	7.5312	1.00	0.054
π C5-C6 → π* C1-C2	39.7062	0.30	0.069
π C5-C6 → π* C3-C4	40.7522	0.28	0.069
n ₁ N7 → π* C1-C2	8.74456	0.31	0.035
n ₁ N7 → σ* C1-C6	12.9704	0.84	0.065
n ₁ F10 → σ* C1-C2	14.6858	0.95	0.073
n ₂ F10 → σ* C2-C3	15.6482	0.93	0.075
n ₂ F10 → π* C1-C2	39.748	0.41	0.087
n ₂ F11 → σ* C2-C3	14.895	0.94	0.073
n ₂ F11 → σ* C3-C4	15.5645	0.93	0.074
n ₃ F11 → π* C3-C4	39.5806	0.41	0.087
n ₂ F12 → σ* C3-C4	15.2298	0.93	0.074
n ₂ F12 → σ* C4-C5	15.3134	0.93	0.074
n ₃ F12 → π* C3-C4	39.2459	0.41	0.087
n ₂ F13 → σ* C4-C5	15.5645	0.93	0.074
n ₂ F13 → σ* C5-C6	14.8532	0.93	0.073
n ₃ F13 → π* C5-C6	38.9949	0.41	0.086
n ₂ F14 → σ* C1-C2	13.8909	0.96	0.071
n ₂ F14 → σ* C5-C6	15.941	0.94	0.076
n ₃ F14 → π* C5-C6	39.4133	0.42	0.088

Conversely, an interaction with a bonding pair as the acceptor may strengthen the bond. Strong electron delocalisation in the Lewis structure also shows up as donor-acceptor interactions. The stabilisation energy of different kinds of interactions are listed Table 9.

This calculation is done by examining all possible interactions between 'filled' (donor) Lewis-type NBOs and 'empty' (acceptor) non-Lewis NBOs, and estimating their energetic importance by 2nd order perturbation theory. Since these interactions lead to loss of occupancy from the localised NBOs of the idealised Lewis structure into the empty non-Lewis orbitals (and thus, to departures from the idealized Lewis structure description), and they are referred to as 'delocalisation' corrections to the natural Lewis structure.

The NBO method demonstrates the bonding concepts like atomic charge, Lewis structure, bond type, hybridization, bond order, charge transfer and resonance weights. Natural bond orbital (NBO) analysis is a useful tool for understanding delocalisation of electron density from occupied Lewis-type (donor) NBOs to properly unoccupied non-Lewis type (acceptor) NBOs within the molecule. The stabilisation of orbital interaction is proportional to the energy difference between interacting orbitals. Therefore, the interaction having strongest stabilisation takes place between effective donors and effective acceptors. This bonding-anti bonding interaction can be quantitatively described in terms of the NBO approach that is expressed by means of second-order perturbation interaction energy $E^{(2)}$ [28]. This energy represents the estimate of the off-diagonal NBO Fock matrix element. The stabilisation energy $E^{(2)}$ associated with i (donor) $\rightarrow j$ (acceptor) delocalisation is estimated from the second-order perturbation approach as given below.

$$E^{(2)} = DE_{ij} = q_i \frac{F(i, j)^2}{\epsilon_j - \epsilon_i}$$

where, q_i is the donor orbital occupancy, ϵ_i and ϵ_j are diagonal elements (orbital energies) and $F(i, j)$ is the off-diagonal Fock matrix element. In the bond pair donor orbital, $\pi_{CC} \rightarrow \sigma^*_{CC}$ interaction between the C3-C4 bond pair and the antiperiplanar C1-C2 antibonding orbital give stabilisation of 38.451 kJ mol⁻¹ for PFA. The bond pair donor orbital, $\sigma_{CC} \rightarrow \sigma^*_{CF}$ interaction between the C1-C6 bond pair and the antiperiplanar C5-F13 antibonding orbital give stabilisation of 7.44752 kJ mol⁻¹ for PFA. The 252 lone pair donor orbital, $n_F \rightarrow \pi^*_{CC}$ interaction between the F10 carbon lone pair and the antiperiplanar C1-C2 antibonding orbital is seen to give a strong stabilisation, 39.748 kJ mol⁻¹ for PFA. The lone pair donor orbital, $n_N \rightarrow \sigma^*_{CC}$ interaction between the N7 lone pair and the antiperiplanar C1-C6 antibonding orbital is seen to give stabilisation, 12.9704 kJ mol⁻¹ for PFA. The Fig. 5 shows that local negative electrostatic potentials (red) signal for C atoms with lone pairs whereas local positive electrostatic potentials (blue) signal for NH₂ atoms for PFA.

Magnetic Susceptibility

Atoms are free radicals in ions which contain one or more unpaired electron will possess permanent magnetic dipole moment, that arises from the spin residual spin and angular momentum of the unpaired electrons. All substances having permanent magnetic moment display paramagnetic behavior in nature. When a paramagnetic substance is placed in a magnetic field, they will align themselves in the direction of the field and thus produces + magnetic susceptibility, which depends on the temperature; since thermal agitation will

oppose the alignment of the magnetic dipoles.

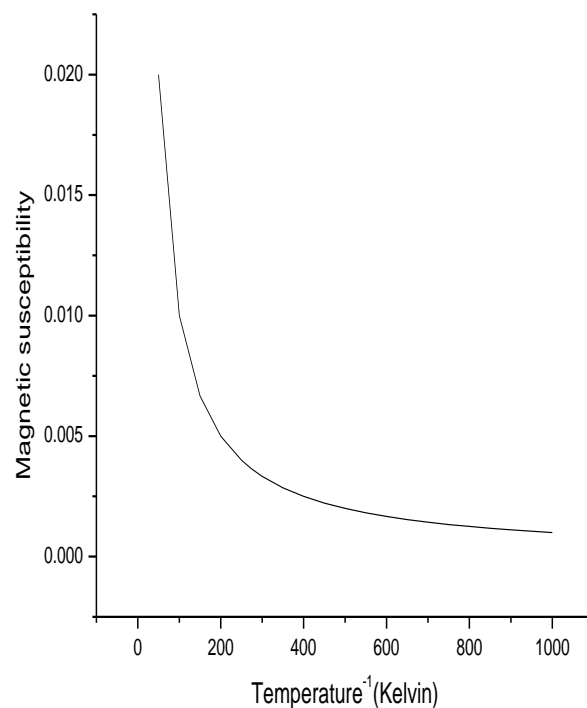


Fig 6 .Graphical representation of magnetic susceptibility with temperature⁻¹

The effectiveness of the field diminishes with increase in temperature. The magnetic susceptibility (χ_m) of the molecules for various temperatures are predicted with the unpaired electron and presented in Table 10. The representation of graphical(χ_m) method with 1/T (temperature⁻¹) is shown in Fig. 6. The effective magnetic moment is found to be a constant, which is 1.9647×10^{-5} (BM) and the Curie constant is obtained from the magnetic moment (μ_m) and is found to be 4.9910×10^5 .

Table10. Magnetic susceptibility of 2,3,4,5,6-pentafluoroaniline by B3LYP/6-311+G(d,p).

Temperature	Magnetic susceptibility	1/Temperature
50	6.32568E-07	0.02
100	7.48622E-07	0.01
150	9.23418E-07	0.006667
200	7.52368E-07	0.005
250	5.26792E-07	0.004
273	4.12564E-08	0.003663
298.15	4.98342E-08	0.003354
300	3.25825E-08	0.003333
350	1.54398E-08	0.002857
400	1.34567E-08	0.0025
450	9.15432E-08	0.002222
500	5.74450E-10	0.002
550	4.67545E-10	0.001818
600	7.67564E-10	0.001667
650	6.82568E-10	0.001538
700	9.48622E-10	0.001429
750	4.13498E-11	0.001333
800	5.72748E-11	0.00125
850	3.56927E-11	0.001176
900	8.74735E-11	0.001111
950	5.67859E-11	0.001053
1000	9.12567E-11	0.001

Temperature Dependence of Thermodynamic Properties

The temperature dependence of the thermodynamic properties namely heat capacity at constant pressure (C_p), heat capacity (C_v), entropy (S), internal heat (U), Gibb's free energy (G) and enthalpy change (H) for the compounds NCF were determined by B3LYP/6-311++G(d,p) method. Fig. 7 depicts the correlation of heat capacity at constant pressure (C_p), Gibb's free energy (G), entropy (S) with temperature by B3LYP/6-311++G(d,p) method. Table 11 reveals that the entropies, heat capacities, constant pressure, internal heat Gibb's free energy and enthalpy changes are increasing with temperature ranging from 10 to 500 K due to the fact that the molecular vibrational intensities increases with temperature [29]. The regression factors (R_2) of these observed relations of the thermodynamic functions vs. temperatures are all not less than 0.999. For the thermal energy, the regression coefficient (R_2) is 0.987. The correlation equations for the thermodynamic parameters with temperature are given in the graphs. These equations are used to predict the value of any thermodynamic parameters for any temperature.

$$(C_p) = -11E+06x^2 + 0.301x + 2.201$$

$$(S) = 3E+09x^2 + 0.494x + 13.66$$

$$(G) = 3E+09x^2 + 0.0929x + 23.66$$

The molecular structural parameters, thermodynamic properties and fundamental vibrational frequencies of the optimized geometry of PFA, have been obtained from *ab initio* HF and DFT calculations. The theoretical results are compared with the experimental results. Although both types of calculations are useful to explain vibrational spectra of PFA, *ab initio* calculations at HF/6-31+G(d,p) level, it is found a little poorer than DFT/ B3LYP/6-31+G(d,p) level calculations. On the basis of agreement between the calculated experimental results, assignments of all the fundamental vibrational modes of PFA have been made for the first time in this investigation.

Conclusion

The TED calculation regarding the normal modes of vibration provided a strong support for the frequency assignment. Therefore, the assignments proposed at higher level of the theory with higher basis set with only reasonable deviation from the experimental values seems to be correct. Furthermore, the thermodynamic, nonlinear optical, first-order hyperpolarizabilities and total dipole moment properties of the compounds have been calculated in order to get insight into the compound. And also HOMO and LUMO energy gap explains the eventual charge transfer interaction taking place within the molecules. The NBO analysis has been performed in order to elucidate charge transfers or conjugative interaction, the intra-molecule rehybridization and delocalization of electron density within the molecule and bond pair donor orbital, $\pi_{CC} \rightarrow \pi^*_{CC}$ interaction between the C5–C6 bond pair and the C3–C4 antibonding orbital give more stabilisation of 40.7522 kJ mol⁻¹ for PFA. Thermodynamic properties in the range from 10 to 500 K are obtained. The paramagnetic behavior of the molecule under consideration has been investigated and the variation of paramagnetic susceptibility with temperature has been studied.

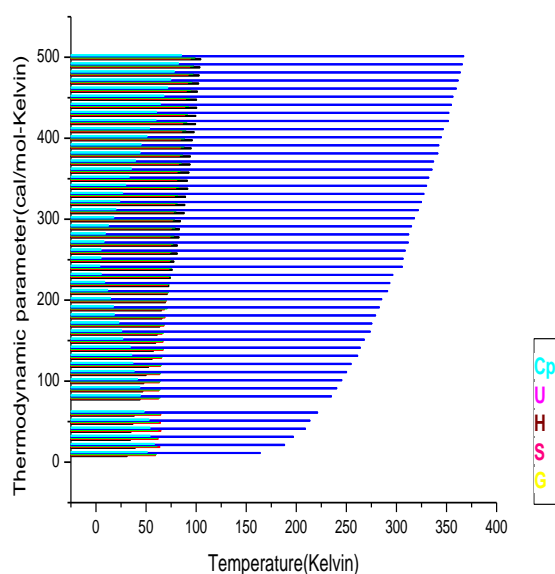


Fig 7. Correlation graphic of thermodynamic parameters and Temperature for entropy (S), heat capacity at constant pressure (C_p), Gibb's free energy (G) energy change of 2,3,4,5,6-pentafluoroaniline

Table 11. Thermodynamic functions of 2,3,4,5,6-pentafluoroaniline determined at different temperatures with B3LYP/6-311+G(d,p) level

Temperature (K)	C _v (J/K/mol)	C _p (J/K/mol)	U (kJ/mol)	H (kJ/mol)	S (J/K/mol)	G (kJ/mol)	Q	ln(Q)
10.000	21.503	30.052	54.505	62.038	162.033	50.056	5.30991E+06	17.2522
20.000	22.002	36.106	60.706	62.856	186.390	58.165	9.82568E+07	17.2950
30.000	24.028	36.342	62.961	64.126	196.097	57.023	4.79622E+08	19.5643
40.000	24.470	33.997	63.809	64.987	209.167	53.965	2.43618E+09	21.6321
50.000	25.105	34.007	64.431	65.798	214.666	53.061	4.58697E+09	21.7005
60.000	30.094	35.262	64.710	65.992	220.376	48.027	8.67820E+09	23.7888
80.000	31.477	40.071	62.675	65.998	236.180	44.267	3.94980E+10	23.9990
90.000	32.912	41.823	62.986	65.988	244.409	48.823	5.90732E+10	24.5200
100.000	40.234	41.745	63.232	66.069	245.480	40.448	9.89225E+10	25.0007
110.000	41.039	52.042	63.649	66.562	253.259	38.026	1.66498E+11	25.5050
120.000	44.059	52.439	64.222	67.099	254.811	38.903	1.69948E+11	27.9998
130.000	45.939	53.005	65.432	67.987	261.393	30.800	2.50060E+11	27.2713
140.000	51.966	54.455	65.997	67.945	263.868	34.231	3.59900E+11	28.9956
150.000	51.424	58.739	66.987	67.481	267.961	26.821	5.66665E+11	29.3423
160.000	53.002	60.231	66.103	68.441	275.889	25.785	7.96560E+11	29.6663
170.000	55.531	61.840	68.884	68.060	275.580	23.009	1.07893E+12	29.9288
180.000	57.587	64.988	68.906	68.533	279.220	18.286	1.99195E+12	30.8768
190.000	59.789	64.441	68.445	70.993	284.981	17.565	1.89008E+12	29.7773
200.000	61.127	68.449	70.990	70.094	285.408	11.600	4.60569E+12	29.8655
210.000	61.470	70.015	73.069	72.419	291.226	11.713	7.31947E+12	31.2341
220.000	63.691	72.768	73.342	72.992	293.487	4.790	4.86567E+12	32.9754
230.000	66.030	74.175	73.766	73.988	296.455	6.307	6.66798E+12	29.8851
240.000	69.973	76.110	73.954	74.888	305.926	3.878	8.45635E+12	29.7225
250.000	69.452	77.886	73.527	74.314	306.729	5.018	5.99223E+13	33.9851
260.000	70.879	81.194	73.763	75.009	308.869	5.044	1.66677E+13	33.6466
270.000	72.076	81.223	74.922	76.998	311.945	8.111	5.99113E+13	34.8805
280.000	73.219	84.996	74.009	77.787	313.331	9.438	2.88970E+13	34.9033
290.000	70.095	84.404	75.283	78.941	316.178	15.595	2.72009E+13	35.8443
300.000	76.414	84.328	76.519	78.456	318.051	16.771	3.98535E+13	35.9921
310.000	77.701	87.015	77.314	79.805	321.879	17.906	4.77577E+13	36.6670
320.000	78.940	87.755	78.725	80.985	324.988	20.709	6.51450E+13	36.8177
330.000	82.384	87.520	78.300	82.455	327.465	21.691	7.55882E+13	37.9775
340.000	86.933	93.685	79.756	82.488	330.111	25.780	9.45640E+13	37.9177
350.000	86.085	93.225	80.769	83.600	332.422	30.143	1.07499E+14	37.9723
360.000	83.828	94.967	81.157	84.080	335.546	31.411	1.80367E+14	37.3452
370.000	87.623	94.999	82.566	84.209	338.190	34.578	1.87188E+14	38.9950
380.000	87.599	95.275	83.599	85.509	343.401	40.109	2.23399E+14	38.5644
390.000	87.899	96.056	84.332	85.899	343.432	42.086	2.39901E+14	38.9924
400.000	88.677	97.099	84.566	86.222	345.834	50.026	6.65043E+14	39.7885
410.000	88.282	98.977	85.600	87.721	345.799	53.492	6.09729E+14	39.4650
420.000	93.677	98.514	86.609	91.664	352.796	59.980	6.59400E+14	39.4459
430.000	94.923	99.729	89.668	91.415	352.405	64.493	7.07208E+14	40.0398
440.000	95.999	101.624	89.790	92.386	354.973	64.291	7.63189E+14	40.6444
450.000	96.734	101.522	89.401	92.427	357.540	69.876	8.06609E+14	40.2294
460.000	96.879	102.245	92.298	95.546	357.780	70.685	5.47006E+15	41.8234
470.000	97.977	103.549	92.655	95.736	364.694	71.715	5.93822E+15	42.9645
480.000	97.696	103.999	93.187	97.996	364.779	72.255	5.99459E+15	43.9881
490.000	97.665	104.800	94.768	97.320	368.824	80.418	5.46265E+15	45.5634
500.000	99.916	105.656	95.345	99.719	368.232	82.456	5.25678E+15	45.9640

Reference

- [1] F.A. Diaz, C.O. Sanchez, M.A. Del Valle, J.I. Torres, L.H. Tagle, *Synth. Met.*, 118 (2001) 25.
- [2] S.C. Ng, L. Xu, *Adv. Matter*, 10 (1998) 1525.
- [3] R.A. Misra, S. Dubey, B.M. Prasad, D. Singh, *Indian J. Chem, sect A*, 38 (1999) 141.
- [4] V. Prevost, A. Petit, F. Pla, *Synth. Met.*, 104 (1999) 79.
- [5] M. Kanungo, A. Kumar, A.Q. Contractors, *Electroanal J. Chem.*, 528 (2002) 46.
- [6] Y. Dong, Mu, *Electrochem Acta* 36 (1991) 2015.
- [7] D.M. DeLong champ, P.T. Hammond, *Chem. Mater*, 16 (2004) 4799.
- [8] R.G. Parr, W. Yang, *Density Functional Theory of Atoms and Molecules*, Oxford University Press, New York, 1989.
- [9] P. Pulay, G. Forgarasi, X. Zhou, P.W. Taylor, *Vib. Spectrosc.*, 1 (1990) 159.
- [10] H.A. Kramers, W. Heisenberg, *J. Phys.* 31 (1925) 681.
- [11] J.M.L. Martin, C.V. Alsenoy, *J. Phys. Chem.* 100 (1996) 6973.
- [12] J.M.L. Martin, J.E.I. Yazal, J.P. Francis, *J. Phys. Chem.* 100 (1996) 15358.
- [13] M.J. Frisch, G.W. Trucks, H.B. Schlegel, *GAUSSIAN 09*, Revision A.02, Gaussian, Inc., Wallingford, CT, 2009.
- [14] C. Lee, W. Yang, R. G. Parr, *Phys. Rev. B* 37 (1988) 785.
- [15] T. Sundius, *J. Mol. Struct.*, 218 (1990) 321.
- [16] T. Sundius, *Vib. Spectrosc.*, 29 (2002) 89.
- [17] MOLVIB (V.7.0): Calculation of Harmonic Force Fields and Vibrational Modes of Molecules, QCPE Program No. 807 (2002).
- [18] A. Frisch, A.B. Nielson, A.J. Holder, *Gaussview User Manual*, Gaussian Inc., Pittsburg, PA, 2000.
- [19] P.L. Polavarapu, *J. Phys. Chem.* 94 (1990) 8106.
- [20] G. Keresztury, Raman spectroscopy theory, in: JM Chalmers, P, R. Griffiths (Eds.), *Handbook of Vibrational Spectroscopy*, Vol. 1, John Wiley & Sons Ltd., 2002, p. 71.
- [21] G. Keresztury, S. Holly, J. Varga, G. Besenyi, A.Y. Wang, J.R. Durig, *Spectrochim Acta part 49A* (1993) 2007.
- [22] M. Fukuyo, K. Hirotsu, T. Higuchi, *Acta Cryst.* 38B, (1982) 640.
- [23] M. Gdaniec *Acta Cryst.* E63, o2954.
- [24] G. Fogarasi, P. Ulay, in: J.R. Durig (Ed.) *Vibrational Spectra and Structure*, Vol.14, Elsevier, Amsterdam, 1985, P. 125, Chapter 3.
- [25] K. Sambathkumar, *Density Functional Theory Studies of Vibrational Spectra, Homo- Lumo, Nbo and Nlo Analysis of Some Cyclic and Heterocyclic Compounds* (Ph.D. Thesis), Bharathidasan University, Tiruchirappalli, August 2014.
- [26] K.Sambathkumar, S.Jeyavijayan, M.Arivazhagan *Spectrochim Acta A* 147 (2015)51-66.
- [27] D.Cecily Mary Glory, R.Madivanane and K.Sambathkumar *Elixir Comp. Chem.* 89 (2015) 36730-36741.
- [28] Kuppusamy Sambathkumar *Spectrochim. Acta A* 147 (2015) 51-66.
- [29] V. Balachandran, S. Rajeswari, S. Lalitha *Spectrochim. Acta A* 124 (2014) 277-284.
- [30] M. Gdaniec *Acta Cryst.* E63, o2954.